Desalination and Water Treatment
www.deswater.com

doi: 10.5004/dwt.2019.23436

142 (2019) 279–292
February

Biosorption of Cu(II) from aqueous solutions by the residues of cider vinegar as new biosorbents: comparative study with modified citrange peels

Meriem Turkman*, Nadji Moulai-Mostefa, Yamina Zouambia

Material and Environmental Laboratory, University of Medea, Ain D'Heb, 26001 Medea, Algeria, Tel./Fax: +213 560 795 520; email: turkmedea@gmail.com

Received 30 May 2018; Accepted 5 November 2018

ABSTRACT

In this work, the synthesis of new biosorbents based on cider vinegar residues (CVR) and modified citrange peels (MCP) and their capacities to remove copper cations (Cu(II)) from aqueous solutions were investigated. Fourier transform infrared (FTIR) spectra, scanning electron microscopy coupled with energy dispersive X-ray analysis, and determination of the zero point of charge (pH_{pzc}) have been employed to determine the physicochemical characteristics of biomasses. It was found that biosorption efficiencies of Cu(II) toward CVR and MCP depend on particle size (from 0.315 to 0.4 mm), biosorbent content (10 g L^{-1}), medium pH (pH = 5), agitation speed (150 rpm), initial concentration of metal ions (200 mg L^{-1}), temperature (25°C), and contact time (3 h). FTIR analysis confirmed the presence of carboxyl and hydroxyl groups in both absorbents and their implications in the metal bond. It was noticed that the pseudo-second-order model fitted well the kinetic of Cu(II) sorption on CVR and MCP with lower values of the normalized standard deviation (10.48% for CVR and 11.6% for MCP). The maximum biosorption capacities according to Langmuir model were 63.92 and 44.92 mg g^{-1} for CVR and MCP, respectively. The average free energies calculated by the nonlinear method of Dubinin-Radushkevich model were found to be 9.64 and 19.38 kJ mol^{-1} for CVR and MCP, showing that the mechanism of biosorption of Cu(II) could be chemical by ion exchange and particle diffusion.

Keywords: Copper; Cider vinegar residues; Modified citrange peels; Biosorption; Kinetic modeling

1. Introduction

The wastewater contamination is a worldwide environmental and social problem. It was estimated for the year 2025 that 4–5 billion people on earth will be living in scarce clean water areas [1]. Among all water pollutants, heavy metals have received a major concern due to their toxicity and persistence and to the fact that they cannot be decomposed in-situ by biological means [2,3].

Copper is one of the most common heavy metals found in aquatic environment [4,5]. It is considered as a micronutrient at low doses since it can hemostatically regulate the trace in the human body. Nevertheless, it is toxic at higher concentration because of its tendency to accumulate in the vital organs [6] causing many diseases and disorders as mental and neurological illnesses, memory loss, cancer [7], etc.

Several techniques such as reverse osmosis, ion exchange, complexation, assisted-ultrafiltration, and adsorption have been widely used for the treatment of water polluted by Cu(II) ions [8–12]. Over the last three decades, adsorption was the most employed method; it is economical, inexpensive, and simple and has a high efficiency in comparison with other conventional techniques [13,14].

In this context, many studies related to the synthesis of low-cost adsorbents from inexpensive materials, essentially agricultural products, were carried out [15]. Among them, biomaterials as apples, citrus peels, mandarin peels, waste

---

* Corresponding author.

1944-3994/1944-3986

activated sludge, sugar beet pectin, banana peel, soya bean hulls, walnut hulls, and bael fruit shells were proposed for the treatment of water charged with heavy metals [16–23]. A recent work [24] reported that the capacities of biosorption of fruit peels in eliminating Cu(II) by adsorption remain comparable with the results found with activated carbon. However, there is a lack of information on the biosorption mechanism and the metal binding phenomena on the surface of fruit peels or apple residues [24–26].

This study, therefore, proposes the utilization of new biosorbents based on cider vinegar residues (CVR) and their comparison with modified citrange peels (MCP) for the treatment of water polluted by copper. It must be mentioned that the north of Algeria is known for its abundance of apples and citrus. In 2013, a quantity of 455,937 tons was produced [27].

Furthermore, apples are used in the manufacture of cider vinegar where large quantities of waste are produced [26]. These wastes are not exploited industrially up to date at the national level, particularly in water purification field. On the other hand, the citrange is very abundant, and its industrial transformation would produce more waste than other fruit peels. Hence, this work aims at exploiting these local residues in the environmental technology, especially in the treatment of contaminated water.

The main objective was to evaluate the biosorption capacity of copper by both CVR and MCP and to examine the impact of particle size, biosorbent content, pH, agitation, and time of contact on the efficiency of biosorption. Moreover, the nonlinear forms of kinetics and equilibrium models were employed to fit experimental data. For the evaluation of the mechanisms of Cu(II) removal by CVR and MCP, the models of Temkin and Dubinin-Radushkevich (D-R) were used. For the determination of the main functional groups implicated in copper biosorption onto biosorbents, a comparative study of Fourier transform infrared (FTIR) spectra after and before biosorption was carried out. Biosorbent morphology was examined by scanning electron microscopy and energy dispersive X-ray spectroscopy.

2. Materials and methods

2.1. Solutions

The reagents used ($CuSO_4·5H_2O$, HCl, NaOH, ammonia) were purchased from Sigma-Aldrich and Merck (Switzerland). The stock sample of Cu(II) at 1 g L^{-1} was obtained by dissolution of analytical grade copper sulfate ($CuSO_4·5H_2O$, Sigma-Aldrich, purity 99%) in distilled water. Solutions of 0.1M HCl (purity 37%, Merck) and 0.1M NaOH (purity 98%, Merck) were prepared by diluting stock solutions of these reagents to adjust the pH.

2.2. Preparation of biosorbents

2.2.1. Preparation of MCP

The citrange fruits were harvested at the end of maturity in the region of Ain D'Heb (Medea, Algeria). The peels were washed with distilled water and then cut into small pieces before being dried until they get a constant mass. After mechanical grinding and sieving, an amount (100 g) of the obtained dried products was chemically treated by 1 L of sodium hydroxide solution at a concentration of 0.1M [28] for 48 h at ambient temperature (25°C ± 5°C). The product supports obtained after decantation and filtration were washed with distilled water until neutral pH (pH = 7) and then dried in an oven at 50°C. The MCP were stored in darkness in tinted glass vials prior to their use.

2.2.2. Isolation of CVR

The CVR were obtained after the vinegar extraction which was performed by apple fermentation at room temperature (25°C–30°C) in closed systems for three months. The obtained residues were dried in the open air for 6 d until a constant weight was obtained and then stored in darkness in tinted glass vials prior to their use.

2.3. Characterization of the prepared biosorbents

The evaluated properties are real and bulk densities, humidity, organic and inorganic matters, and pH of biosorbent suspensions. Determination of the specific surface areas was done by the method previously described by Dada et al. [29]. The pH was determined by a digital apparatus (Hanna Instruments), while the pH_{PZC} parameter of the different samples was measured by a procedure similar to that described in the work of Khormaei et al. [30]. The process consists in preparing several identical samples by placing 50 mL of 0.01M NaCl solution in a closed capped Erlenmeyer flask. The pH of each solution was adjusted from 2 to 12 by adding either HCl (0.1M) or NaOH (0.1M) solutions. The different samples (50 mL of NaCl solution mixed with 0.15 g of biosorbent) are subjected to agitations (150 rpm) at room temperature. After 48 h under stirring, the final pH of each suspension was measured. The pH_{pzc} represents the point where the pH_{final} versus $pH_{initial}$ curve intercepts the line pH_{final} equal to $pH_{initial}$ [31].

The structural characterization by FTIR spectroscopy was performed by analyzing the obtained transparent pellets (mixture of 1 mg of biomass with 100 mg of KBr) by using a Bruker TensorII spectrometer (Germany) in a range of 400–4,000 cm^{-1} [32]. The morphology of biosorbents was examined by SEM using MicronsPerPixY and energy dispersive spectroscopy operating at 20 and 5 kV, respectively.

2.4. Study of the biosorption of copper ions

Batch biosorption experiments were performed by connecting a series of Erlenmeyer flasks containing specific amounts of biosorbents with volumes of 50 mL of the synthetic copper solution ($CuSO_4·5H_2O$). All the obtained systems, at the indicated temperature and pH, were kept under continuous stirring for 24 h to reach the adsorbent-adsorbate equilibrium. After this, the mixtures were centrifuged at 4,000 rpm for 5 min [28] and each supernatant obtained was analyzed using an UV spectrophotometer (Shumadzu, Japan) at a fixed wavelength (λ = 610 nm) to detect and quantify the copper in solutions [24].

For optimization of particle size, sorption tests were undertaken under fixed conditions (concentration of the copper solution = 200 mg L^{-1}, agitation speed = 150 rpm, temperature = 25°C ± 3°C, pH = 3 ± 0.02, and biomass content = 10 g L^{-1}), while the granulometric ranges were varied using three classes: X_1 = [0.315, 0.4] mm, X_2 = [0.16, 0.2] mm, and X_3 = [0.08, 0.1] mm. The effect of the biosorbent content (ranging from 2 to 12 g L^{-1}) was investigated under the same operating conditions and by using the class of granulometry X_1. Effect of pH was evaluated in the range of 2.0–6.0 using biosorbent content of 10 g L^{-1}. The agitation speed was varied between 150 and 800 rpm. The impact of contact time on the retention efficiency on both biosorbents was studied using the same conditions while the stirring speed was adjusted at 150 rpm. The effect of the initial amount of copper in the solution was evaluated between 200 and 1,000 mg L^{-1}. This concentration range was used in the isotherm study.

The sorption capacity, expressed in milligrams of Cu^{2+} per gram (g) of biosorbent, is calculated by the following formula [33]:

$$q = \frac{\left(C_0 - C_e\right)V}{m} \tag{1}$$

And the sorption yield (R) is deduced by Eq. (2):

$$R\left(\%\right) = \frac{\left(C_0 - C_e\right)}{C_0} \times 100 \tag{2}$$

where C_0 and C_e are the concentrations (mg L^{-1}) of Cu^{2+} ions in solutions at t = 0 and at equilibrium, V is the volume (L) of the biosorbent suspension, and m is the mass (g) of the biosorbent used.

2.5. Statistical analysis

All experiments were repeated three times under the same operating conditions. Data analysis was performed based on variance analysis using Origin Pro 9.0 software. Separation of means and/or significant comparisons of all parameters were analyzed by the Tukey test. The significance level used for all statistical tests was 5%. Each data value is the average of the number of repeated ± the absolute error.

2.6. Kinetic modeling

2.6.1. Pseudo-first and pseudo-second orders

The pseudo-first-order kinetic model (Lagergren model) is expressed by Eq. (3) [34]:

$$\frac{dq_t}{dt} = K_1\left(q_e - q_t\right) \tag{3}$$

where q_e and q_t (mg g^{-1}) are the sorption capacities at equilibrium and at time t, K_1 (L min^{-1}) is the rate constant for the pseudo-first-order kinetic.

The nonlinear form of Eq. (3) is as follows [35]:

$$q_t = q_e\left(1 - \exp^{-K_1 t}\right) \tag{4}$$

The reaction rate of the pseudo-second-order reaction depends on the quantity adsorbed on the surface of the adsorbent and on that adsorbed at equilibrium. The pseudo-second-order kinetic equation obeys to Eq. (5) [34]:

$$\frac{dq_t}{dt} = K_2\left(q_e - q_t\right)^2 \tag{5}$$

The nonlinear form of Eq. (5) is given by:

$$q_t = \frac{K_2 q_e^2 t}{1 + K_2 q_e t} \tag{6}$$

The constants of pseudo-first-order and pseudo-second-order models were determined by the nonlinear regression using the software Origin Pro9.

In order to compare the application of each model, the normalized standard deviation Δq (%) was evaluated [35]:

$$\Delta q\left(\%\right) = 100 \times \sqrt{\frac{\sum\left[\left(q_{t,\exp} - q_{t,\mathrm{cal}}\right) / \mathrm{q}_{t,\exp}\right]^2}{\left(n-1\right)}} \tag{7}$$

where $q_{t,\exp}$ and $q_{t,\mathrm{cal}}$ are the experimental and calculated sorption capacities at time t and n is the number of data points.

2.6.2. Intraparticle diffusion model

The diffusion of copper ions in different types of biosorbents was investigated using the model of Weber and Morris [36]:

$$q_t = K_{\mathrm{int}} t^{0.5} + X_i \tag{8}$$

where K_{int} is the constant of the Weber intraparticle diffusion (mg g^{-1} min$^{0.5}$), q_t is the quantity adsorbed at time t (mg g^{-1}), X_i represents the value of the thickness of the boundary layer, and t the time (min).

The plot of q_t versus $t^{0.5}$ suggests that the model of intraparticle diffusion governs the biosorption kinetics.

2.7. Sorption isotherms

Sorption isotherms (equilibrium data) are the main requirements to understand the sorption mechanisms [12]. In this investigation, several models were used (Langmuir, Freundlich, Temkin, and D-R).

When the sorption is done in a single layer, in strongly equivalent sorption sites which can contain only one molecule per site and that there are no interactions between the sorbed molecules, the nonlinear form of Langmuir model will be the most appropriate to describe the experimental isotherms [37]:

$$q_e = \frac{K_L \times q_m C_e}{1 + K_L C_e} \tag{9}$$

where C_e is the equilibrium concentration (mg L^{-1}), q_e is the equilibrium sorbed amount (mg g^{-1}), $q_{\max}$ is the maximum sorbed amount at saturation of the monolayer or the maximum sorption capacity (mg g^{-1}), K_L is the Langmuir equilibrium constant (L mg^{-1}).

The viability of the phenomenon of adsorption can still be defined from the dimensionless separation factor R_L given by Eq. 10 [38]:

$$R_L = \frac{1}{\left(1 + K_L C_0\right)} \tag{10}$$

Thus, the sorption is favored for values of $R_L < 1$, poor when $R_L > 1$, and irreversible if $R_L = 0$.

The empirical model of Freundlich is simple and remains the most commonly used; it can be employed in many cases, in particular the multilayer sorption with possible interactions between the sorbed species [38].

$$q_e = K_F \times C_e^{1/n} \tag{11}$$

where K_F represents a constant relative to the sorption capacity in mg$^{(1-n)}$ L^n g^{-1}.

The Temkin model is based on the assumption that during sorption in the gas phase, the adsorption heat decreases linearly with the recovery rate θ due to interactions with the sorbate. It is an application of the Gibbs relation for sorbents whose surface is considered energetically homogeneous. Nowadays, several authors [29] propose the use of this model in liquid phase by plotting q_e or θ according to lnC_e.

$$\frac{q_e}{q_{\max}} = \frac{RT}{\Delta Q} \times \ln\left(K_T \times C_e\right) \tag{12}$$

where ΔQ represents the sorption energy variation (J mol^{-1}) and K_T is the Temkin constant.

The nature of biosorption of copper ions (chemisorption or physisorption) is determined by employing D-R model. This model is given by Eq. 13 [29]:

$$q_e = q_m\mathrm{DRe}^{-\left(B\varepsilon^2\right)} \tag{13}$$

where $q_{m\mathrm{DR}}$ is the maximum sorption capacity and B is the constant related to the sorption energy described by Eq. 14:

$$E = \frac{1}{\left(2\mathrm{B}\right)^{0.5}} \tag{14}$$

The term ε can be correlated as

$$\varepsilon = RT \times \ln\left(1 + \frac{1}{C_e}\right) \tag{15}$$

The constants of the models of Langmuir, Freundlich, Temkin, and that of D-R were also determined by the nonlinear regression using the software Origin Pro9.

3. Results and discussion

3.1. Characterization of the biosorbents used

3.1.1. Physicochemical characterization

The main results related to the physicochemical characterization of the prepared biomaterials (CVR and MCP) are gathered in Table 1. The corresponding values show clearly that CVR and MCP adsorbents are moderately hygroscopic with average humidity about 13% and 20%, respectively. These values confirm those suggested by Dutta et al. [39] for citrus peel. In addition, the total pore volumes of CVR and MCP matrices are, respectively, in the order of 0.99 and 0.89, suggesting that the MCP matrix is denser than CVR. Similar results were obtained with activated carbon [40].

The apparent densities (0.55 g cm^{-3} for CVR and 0.69 g cm^{-3} for MCP) are very similar to that of green pea peels which is equal to 0.67 g cm^{-3} obtained by Bhatnagara et al. [41]. The values of specific surface areas are in the order of 58 m^2 g^{-1} for CVR and 109 m^2 g^{-1} for MCP and seem to be very close to those reported previously for certain biosorbents and especially for orange peels [42].

From the chemical analysis (Table 1), it was shown that the organic matter represents the most important fraction with rates up to 70%. It consists mainly of carboxyl and hydroxyl groups, which are important functional groups that are involved in the sorption phenomenon [41].

3.1.2. Structural analysis

FTIR spectra of CVR and MCP biosorbents after and before copper biosorption tests are grouped together in Fig. 1(a) and (b). Analysis of these spectra shows the following phenomena: (1) the biomasses have the main characteristic peaks of polysaccharides which are hydroxyl groups located at 3,200–3,500 cm^{-1}; they correspond to O–H vibration due to the inter- and intramolecular hydrogen bonding of alcohols, phenols, and carboxylic acids of

Table1
Physical and chemical characteristics of the prepared biosorbents

Characteristics	MCP	CVR
C (%, in wt.)	58.41	59.55
O (%, in wt.)	39.27	39.24
Na (%, in wt.)	1.60	–
K (%, in wt.)	0.22	1.21
Ca (%, in wt.)	0.50	–
Humidity (%)	20.17	13.65
d_r (g cm^{-3})	1.82	1.21
d_{app} (g cm^{-3})	0.69	0.55
Total porosity	0.40	0.36
S (m^2 g^{-1})	109.40	58.20
Organic material (%)	69.3	66.7
Mineral matter (%)	10.6	7.2
Total pore volume (cm^3 g^{-1})	0.89	0.99
pH	4.74	4.20
Granulometry (mm)	[0.31–0.40]	[0.31–0.40]

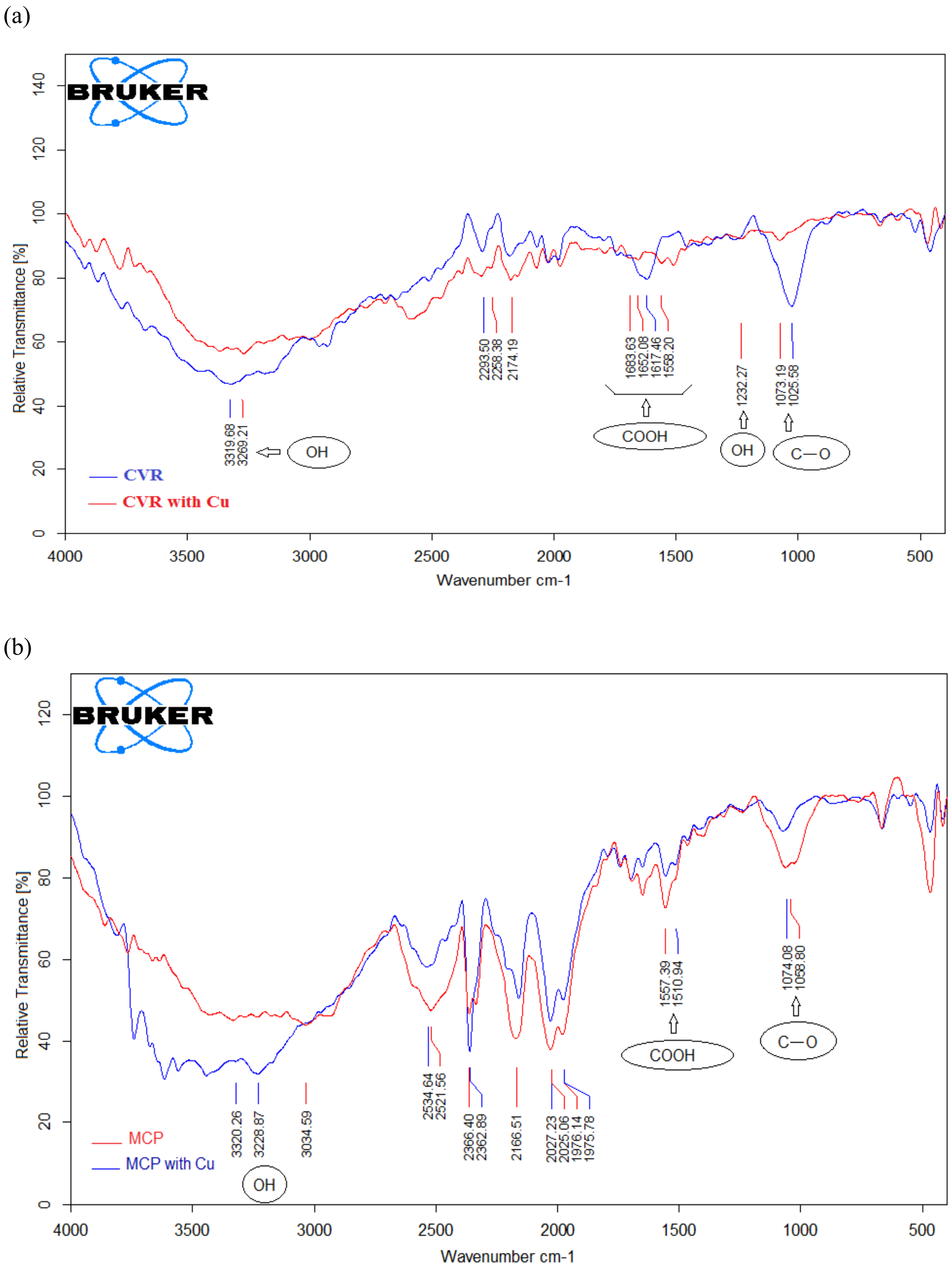

Fig. 1. FTIR spectra of the two studied modified biosorbent samples before and after the sorption of Cu(II): (a) CVR; (b) MCP.

polymeric compounds such as pectin, cellulose, and lignin; (2) the alkyl groups CH and C=O bonds of the carboxylic groups are, respectively, located at 2,850–3,000 cm^{-1} and at 1,500–1,640 cm^{-1} [43]; (3) the peaks expected at 3,319, 1,617, and 1,025 cm^{-1} shifted, respectively, to 3,269, 1,558, and 1,073 cm^{-1} for CVR. However for MCP, the peaks expected at 3,034, 1,557, and 1,058 cm^{-1} shifted, respectively, to 3,228, 1,510, and 1,074 cm^{-1} due to copper sorption. Moreover, the analysis of Fig. 1(a) and (b) shows that the intensity of the peaks in the region between 3,200 and 3,300 cm^{-1} (OH group) decreases after the biosorption of copper ions. The same observation is noted for the region between 1,550 and 1,617 cm^{-1} corresponding to the COOH groups. The significant change in these peaks suggests that chemical interactions between the ions of the metal, hydroxyl (OH), and carboxylic groups occur at the biomass surface; (4) the peak changes that were observed between 1,375 and 1,300 cm^{-1} reflect the symmetric or asymmetric bonding vibrations of the carboxylic groups (–COOH) of pectin; these groups of uronic acid compound provide the ion exchange capacity between pectin and solutes [44].

These results indicate that the mentioned functional groups are mainly implicated in the biosorption of copper on both studied biomasses as suggested by Feng et al. [28] and Lasheen et al. [45].

3.1.3. Morphological analysis

SEM micrographs of both CVR and MCP biosorbents are shown in Figs. 2 and 3. From the exploitation of these micrographs, we note that the surfaces are irregular and porous and consequently have a morphology adapted to the retention of Cu^{2+} ions. The MCP support treated with NaOH appears to be characterized by a more irregular and porous structure in perfect concordance with the observations of Feng et al. [28]. Finally, the mass percentages of the chemical composition of CVR and MCP biosorbents are summarized in Table 1. These results indicate that the proportions of carbon and oxygen are the highest and consequently confirm the organic and acidic nature of these two bio-materials as mentioned earlier by Li et al. [42].

3.2. Optimization of operating parameters

3.2.1. Particle size

The advantage that the granulometric study can present is the ability to choose the best granulometry favoring both sorptive qualities and mechanical properties of the used biosorbent supports [32]. The experimental values of q_e and R (%) parameters of each size class for both the studied biomasses are given in Table 2. The corresponding results show that the bisorption of copper is particularly favored for particles of large sizes. According to the nature of CVR, this remarkable efficiency of X_1 particle size class is attributed to aggregate formation which seems to prevent the migration of Cu(II) ions to the active sites.

For MCP, most of the cationic sites are located inside the pores and the channels and cavities of the MCP. Therefore, the decrease in grain size leads to a decrease in adsorption capacity [46,47].

3.2.2. Biomass content

From the analysis of Fig. 4, representing the yield versus the biomass content, it was noticed that the yield of biosorption of copper ions increases rapidly with the increase of biomass content. Retentions of the order of 7% to 24% and 50% to 86% are obtained, respectively, with CVR and MCP biomasses when their content increases from 2 to 10 g L^{-1}. Beyond this concentration, the yield decreases. The differences between the averages of R (%) for different grades are statistically significant at 5% for CVR and MCP. This may be due to the contact surface involved, where the higher the biosorbent content, the greater the contact surface offered which leads to a gradual increase of sorption sites. These constatations are analogous to those previously reported by Guler and Sarioglu [48] where they choose a content of 10 g L^{-1} as an optimal value.

3.2.3. pH of suspensions

The pH is an essential parameter in the process of biosorption. In fact, it cannot only affect the solubility of metals [20] but also influence the ionization state of the different chemical groups of the used biosorbents. The corresponding results of the yields R (%) and biosorbed quantities q (mg g^{-1}) are summarized together in Table 3. For each pH, the measured values are very close. The small differences found (around 5%) appear statistically insignificant for CVR and MCP, respectively.

It appears from Table 3 that an increase in the pH of the suspension from 2 to 5 influences the copper biosorption. The removal percentage of the metal ions increases from 23% to 45% for CVR and from 48% to 96% for MCP when the pH increases from 3 to 5 but decreases thereafter due to copper precipitation and formation of $Cu(OH)_2$. Thus, at pH 6, there are $Cu(OH)_2$ species that remain the majority compared with the two other minor species, Cu^{2+} and $CuOH^+$ [49]. So, an optimal value of pH (pH = 5) was retained and used for subsequent experiments with CVR and MCP supports.

Indeed, in acidic medium (low pH), the functional groups exist in a protonated form while the charge of the surface of biosorbents is positive, which prevents the fixation of cations (Cu^{2+}) and thus a decrease in the fixing capacity. However, at pH values of 4 and 5, the functional groups become deprotonated (gradual release of protons) and the number of anionic sites is therefore more important that lead to an improvement in the biosorption capacity. Hence, when the pH increases, the total surface of the sorbent became negatively charged. As a consequence, the electrostatic attraction between the positive species (Cu^{2+} ions) and the negative charges of the biosorbent surface sites would lead to an increase in the sorption of the metal ions [42,45]. Studies of the predominant species of Cu^{2+} metal ions as a function of pH have shown that at pH less than 6, the Cu^{2+} ions remain the predominant species and precipitate in $Cu(OH)_2$ form as soon as the pH exceeds the value of 6 [12].

The pH_{pzc} values of CVR and MCP are in the order of 3.25 and 6.5. In the case of MCP, this value is identical to that found by Izquierdo et al. [49] for modified orange peel (pH_{pzc} = 6.52).

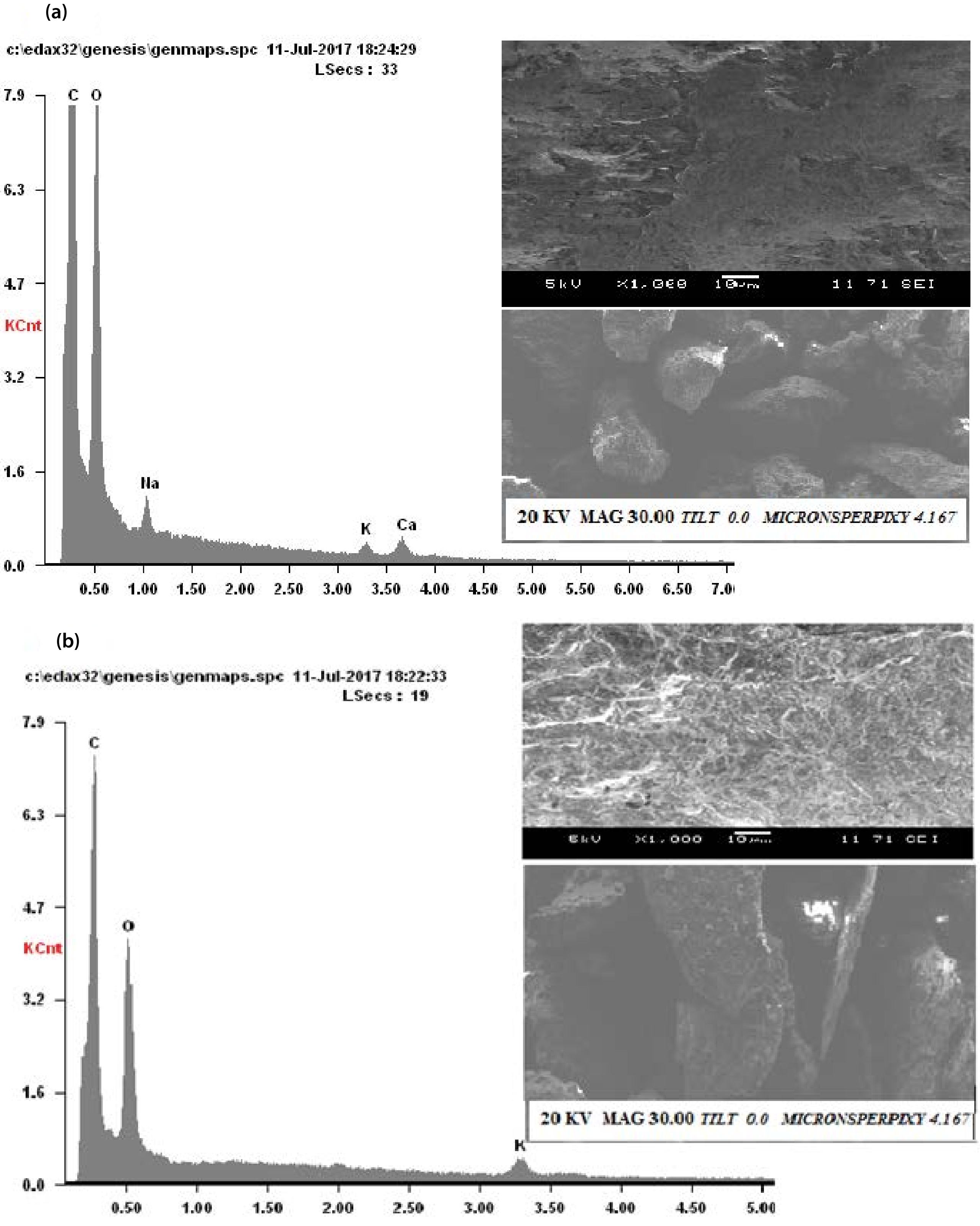

Fig. 2. EDX spectra before biosorption of copper ions: (a) MCP, (b) CVR.

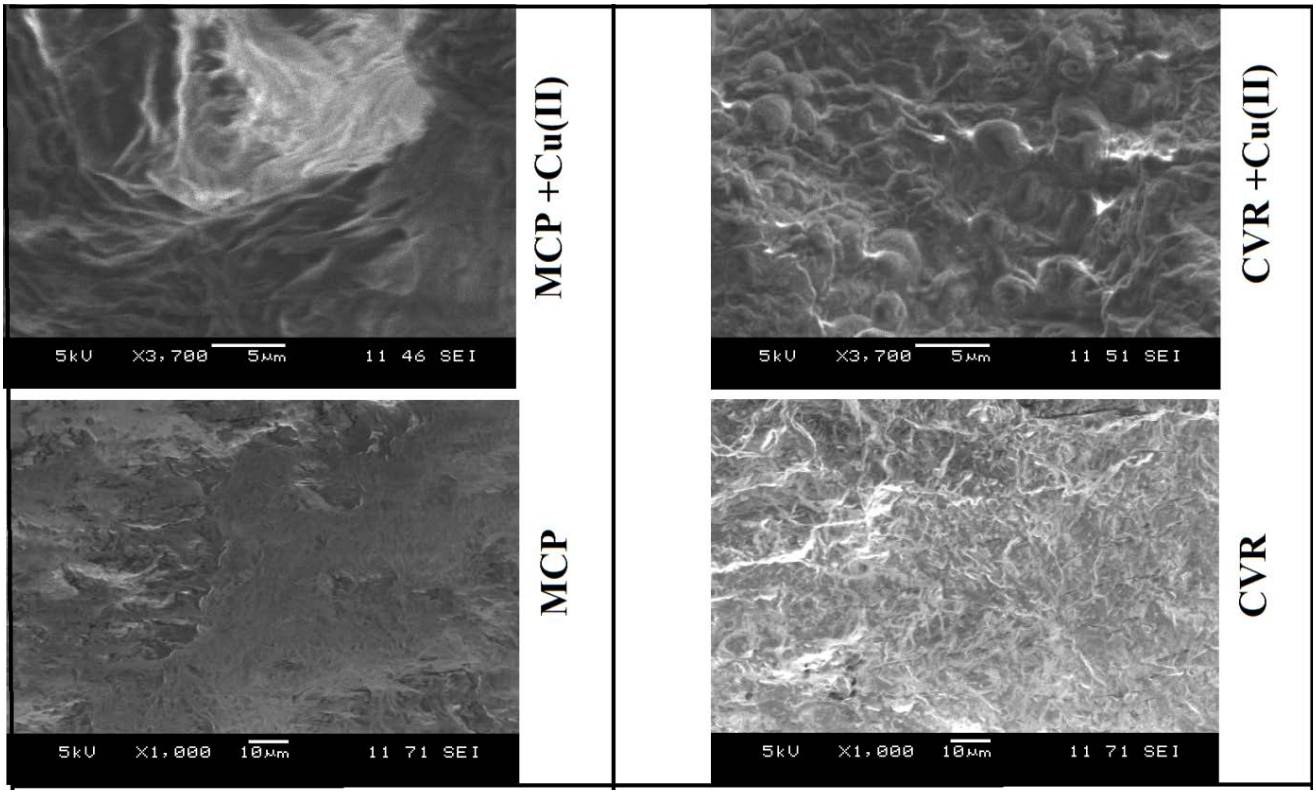

Fig. 3. SEM images for both types of biosorbents before and after Cu(II) biosorption.

Table 2
Effect of particle size of biosorbents on the sorption capacity q (mg g^{-1}) and sorption efficiency R (%) of copper ions

grain size classes (mm)		[0.08–0.1]	[0.16–0.2]	[0.315–0.4]
CVR	q_e (mg g^{-1})	0.11 ± 0.01*a*	0.80 ± 0.19*b*	1.68 ± 0.08*c*
	R (%)	0.58 ± 0.06*a*	4.015 ± 0.95*b*	8.35 ± 0.44*c*
MCP	q_e (mg g^{-1})	14.31 ± 0.10*a*	16.19 ± 0.21*b*	16.85 ± 0.01*c*
	R (%)	62.04 ± 0.44*a*	70.18 ± 0.95*b*	85.87 ± 0.06*c*

Each value is the average of the repeated experiments ± absolute error. The averages followed by different letters in the same line are significantly different at $p < 0.05$.

3.2.4. Agitation speed

The corresponding values in terms of yield and biosorbed quantities are given in Table 4. For MCP, the differences between the averages of stirring speeds (250, 150, and 800 rpm) are not significant at 5%, but the differences between the averages of agitation speeds 250 and 600 rpm and between 600 and 800 rpm are statistically significant at 5%.

Moreover, the decrease in Cu^{2+} ion sorption at a very high speed may be due to the excessive agitation of copper ions in the sorption vessel, so that the repulsive forces predominate at the sorption sites on the sorbent surfaces, which ultimately reduces the attraction between the copper ions and the biosorbent [50]. Hence, a moderate stirring around 150 rpm would support a better homogenization of suspensions; this value was selected as an optimal value (Table 4). It should be noted that similar results for the elimination of various other

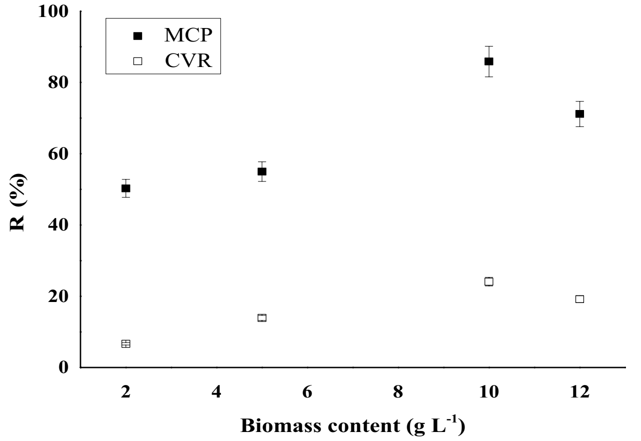

Fig. 4. Influence of the biosorbent content on the biosorption efficiency of Cu^{2+} (C_0 = 200 mg L^{-1}, pH$_{\text{initial}}$ = 3, agitation speed = 150 rpm, T = 25°C, granulometry: [0.31–0.40] mm, t = 24 h).

Table 3
Effect of pH on the sorption capacity q_e (mg g^{-1}) and sorption efficiency R (%) of copper ions by CVR and MCP

pH		2.56–2.73	3.32–3.44	4.04–4.12	5–5.22	5.95–6
CVR	q_e (mg g^{-1})	5.76 ± 0.03*a*	4.77 ± 0.51*a*	8.47 ± 2.14*a*	9.27 ± 0.70*a*	8.37 ± 1.23*a*
	R (%)	28.02 ± 0.18*b*	23.21 ± 2.5*b*	41.17 ± 10.42*b*	45.05 ± 3.42*b*	40.68 ± 5.98*b*
MCP	q_e (mg g^{-1})	7.41 ± 0.38*a*	8.78 ± 0.62*a*	12.01 ± 0.07*b*	17.87 ± 0.01*c*	17.82 ± 0.23*c*
	R (%)	39.83 ± 2.07*a*	48.43 ± 2.07*b*	64.56 ± 0.37*c*	96.04 ± 0.07*d*	95.8 ± 1.24*d*

Each value is the average of the repeated experiments ± absolute error. The averages followed by different letters in the same row are significantly different at $p < 0.05$.

Table 4
Effect of agitation on the sorption capacity q_e (mg g^{-1}) and sorption efficiency R (%) of copper ions

Agitation speed (rpm)		150	250	600	800
CVR	q_e (mg g^{-1})	9.27 ± 0.7*a*	8.85 ± 0.12*a*	5.16 ± 0.09*b*	5.96 ± 0.02*b*
	R (%)	45.05 ± 3.42*a*	40.92 ± 0.53*a*	23.88 ± 0.41*b*	27.55 ± 0.14*b*
MCP	q_e (mg g^{-1})	17.87 ± 0.01*a*	11.07 ± 0.73*b*	9.77 ± 0.1*bd*	8.95 ± 0.13*cd*
	R (%)	96.04 ± 0.07*a*	51.3 ± 3.39*b*	45.28 ± 0.48*bd*	41.49 ± 0.59*cd*

Each value is the average of the repeated experiments ± absolute error. The averages followed by different letters in the same row are significantly different at $p < 0.05$.

heavy metals on some biomaterials were reported by Shroff and Vaidya [38].

3.2.5. Contact time

Fig. 5 shows the effect of contact time on the kinetics of biosorption where it was observed that the process of biosorption of Cu^{2+} is rapid during the first 2 h and reaches a plateau from 70 min for CVR and from 40 min for MCP. The maximum sorption capacities recorded after 1,440 min of contact are in the order of 10 and 18 mg g^{-1} for CVR and MCP, respectively. Similar observations were obtained by Mohamed and Ibrahim [51].

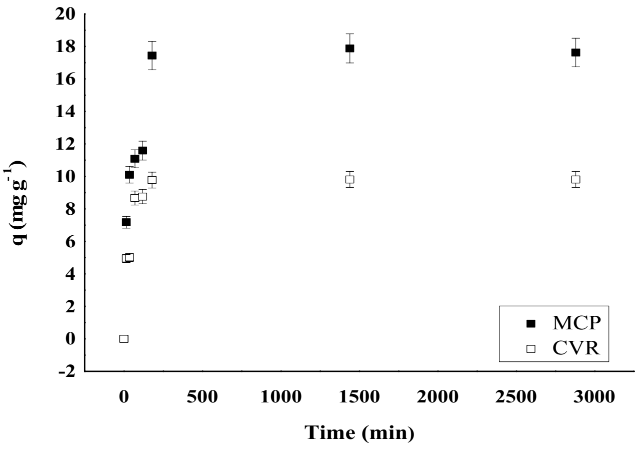

Fig. 5. Effect of contact time on the kinetics of biosorption (C_0 = 200 mg L^{-1}, agitation speed = 150 rpm, T = 25°C, granulometry: [0.31–0.40] mm, pH = 5, biomass content: 10 g L^{-1}).

3.2.6. Initial amount of the metallic solution

According to Fig. 6, it was observed that the sorption increases with increasing concentration of copper solution and tends to approach constant values for both biosorbents at high concentrations. These results indicate that the obtained curves are compatible with the Langmuir isotherm and agree well with those obtained by Feng et al. [28].

3.3. Kinetics modeling

3.3.1. Comparison between the pseudo-first and pseudo-second orders

The parameters of both used models in terms of deduced rate constants calculated biosorbed quantities, and their correlation coefficients are summarized in Table 5 and exploited as curves in Fig. 7. It was observed that the nonlinear form of pseudo-second-order kinetic model is more adequate with lower values of the normalized standard deviation (10.48% for CVR and 11.6% for MCP) in comparison with the values obtained for the pseudo-first-order kinetic model (10.75% for CVR and 16.54% for MCP).

The fixed amounts of Cu^{2+} ions obtained by the pseudo-second-order model reach values of 10.36 and 19.78 mg g^{-1} for CVR and MCP (Table 5). These values approach the experimental results which are in the order of 9 and 18 mg g^{-1} obtained, respectively, with CVR and MCP. Similar observations have been recorded by Lasheen et al. [45] for modified orange peels.

3.3.2. Model of intraparticle diffusion

The curves obtained by the application of the intraparticle diffusion model (Fig. 8) show multilinearity for both

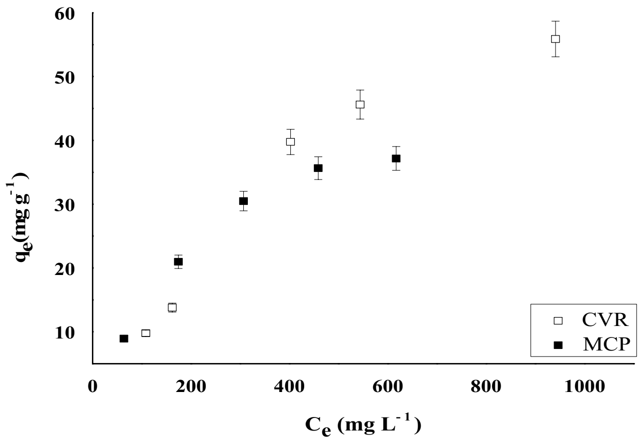

Fig. 6. Effect of the initial concentration of copper ions on the biosorption capacity (pH = 5, agitation speed = 150 rpm, $T = 25°C$, granulometry: [0.315–0.4] mm, biomass content: 10 g L^{-1}, $t = 3$ h).

CVR and MCP matrices indicating that more than one step is implicated in the elimination of Cu^{2+} ions. It can therefore be deduced that the biosorption of Cu^{2+} takes place in two stages: a first step relating to the retention of the cations on the surface of the biosorbent, followed by intraparticle diffusion of Cu^{2+} ions. Same results were reported by Kazmi et al. [52] in their study on the biosorption of Cu^{2+} on the peels of *Prunus amygdalus*.

3.4. Sorption isotherms

For comparative purposes, the values of the corresponding isotherm parameters and their correlation coefficients (R^2) are grouped in Table 6.

The validity of the experimental results is based on the value of R^2. Thus, the closer this coefficient is to unity, the more the results are in adequacy with the considered model [12].

The nonlinear form of the Langmuir isotherm was deduced from Eq. (9) by plotting q_e versus C_e (Fig. 9). According to the obtained results, we note high R^2 for the two biosorbents which are equal to 0.99 for both biosorbents (Table 6). Furthermore, the values of maximum sorption capacity determined by the Langmuir model are equal to 63.92 and 44.92 mg g^{-1} for CVR and MCP (Fig. 9). These values are near the experimental sorption capacities and correspond closely to the adsorption isotherm plateau. So the Langmuir isotherm is well fitted to the equilibrium data. These results justify the utilization of this model.

The nondimensional separation factor R_L is less than unity ($R_L < 1$) for both biosorbents used ($R_L = 0.9$ for CVR and 0.8 for MCP), which would therefore promote the biosorption.

The sorption data for Freundlich isotherm are plotted according to Eq. (11), where q_e is represented as a function of C_e (Fig. 10). The values of R^2 were found equal to 0.98 for both biosorbents.

Besides this, the values of standard error for each parameter obtained by using the Freundlich isotherm model are higher than those obtained by the Langmuir model (Fig. 10).

Table 5
Comparison between the nonlinear forms of pseudo-first-order and pseudo-second-order models

Biosorbent	$q_{e,\text{exp}}$ (mg g^{1})	Pseudo-first order			Pseudo-second order		
		K_1 (mn^{-1})	q_{model} (mg g^{-1})	Δq (%)	K_2 (L (mg mn)$^{-1}$)	q_{model} (mg g^{-1})	Δq (%)
MCP	17.88	0.021	17.58	16.54	0.0015	19.78	11.60
CVR	9.81	0.029	9.55	10.75	0.0038	10.36	10.48

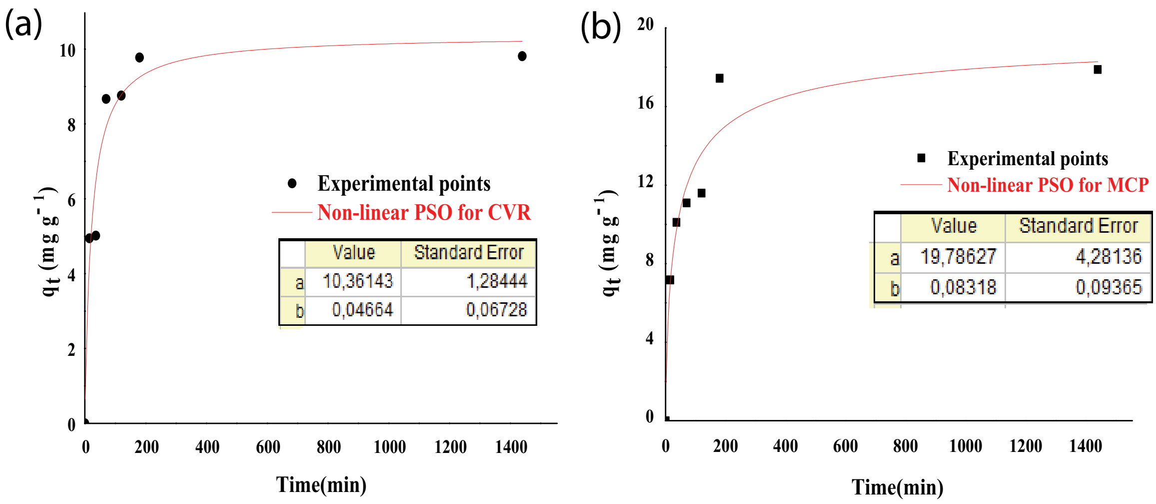

	Value	Standard Error
a	10,36143	1,28444
b	0,04664	0,06728

	Value	Standard Error
a	19,78627	4,28136
b	0,08318	0,09365

Fig. 7. Experimental data and fitted nonlinear form of pseudo-second order (PSO) for the biosorption of copper: (a) q_{model} (mg g^{-1}), (b) ($K_2 \times q_{\text{model}}$) (pH = 5, agitation speed = 150 rpm, $T = 25°C$, granulometry: [0.315–0.4] mm, biomass content: 10 g L^{-1}, $C_0 = 200$ mg L^{-1}).

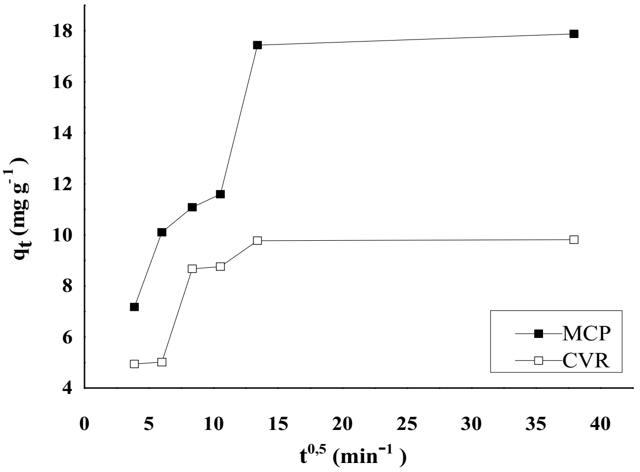

Fig. 8. Intraparticle diffusion model for biosorption of Cu^{2+} on MCP and CVR (pH = 5, agitation speed = 150 rpm, T = 25°C, granulometry: [0.315–0.4] mm, biomass content: 10 g L^{-1}, C_0 = 200 mg L^{-1}).

Consequently, the Freundlich isotherm model cannot generate a satisfactory fit to experimental data [53].

The experimental results of nonlinearization of the Temkin model [Eq. (12)] are presented in Fig. 11. The values of R^2 are equal to 0.99 and 0.83 for MCP and CVR (Table 6). These values indicate that the biosorption process of copper ions can be described by this model.

The variation of the biosorption energy ΔQ resulting from the nonlinearization of the Temkin model is positive (11.31 kJ mol^{-1} for CVR and 8.43 kJ mol^{-1} for MCP) as shown in Table 6. These positive values illustrate that the adsorption reaction of copper ions is endothermic.

On the other hand, the experimental results (Fig. 12) were also found to be consistent with the D-R model (R = 0.93 for CVR and 0.84 for MCP). The parameter B is used to deduce the sorption energy (E). According to the literature [54,55], the following phenomena occur: (1) the physisorption dominates the sorption mechanism when E is between 1 and 8 kJ mol^{-1}, (2) the ion exchange is the main factor when E is between 8 and 16 kJ mol^{-1}, and (3) the sorption is dominated by particle diffusion if E is greater than 16 kJ mol^{-1}.

Table 6
Equation parameters and correlation coefficient for the nonlinear form of isotherms

Isotherms	biosorbents	Constants			
		q_m (mg g^{-1})	$K_L \times 10^4$ (L mg^{-1})	R^2	R_L
Langmuir	MCP	44.92	7.92	0.99	0.80
	CVR	63.92	0.40	0.99	0.90
Freundlich		K_F (mg g^{-1})	n	R^2	
	MCP	53.40	–0.04	0.98	
	CVR	75.75	–0.01	0.98	
Temkin		K_t (L mg^{-1})	ΔQ (KJ mol^{-1})	R^2	
	MCP	0.03	8.43	0.99	
	CVR	0.03	11.31	0.83	
D-R		q_m (mg g^{-1})	E (KJ mol^{-1})	R^2	
	MCP	34.81	19.38	0.84	
	CVR	53.08	9.64	0.93	

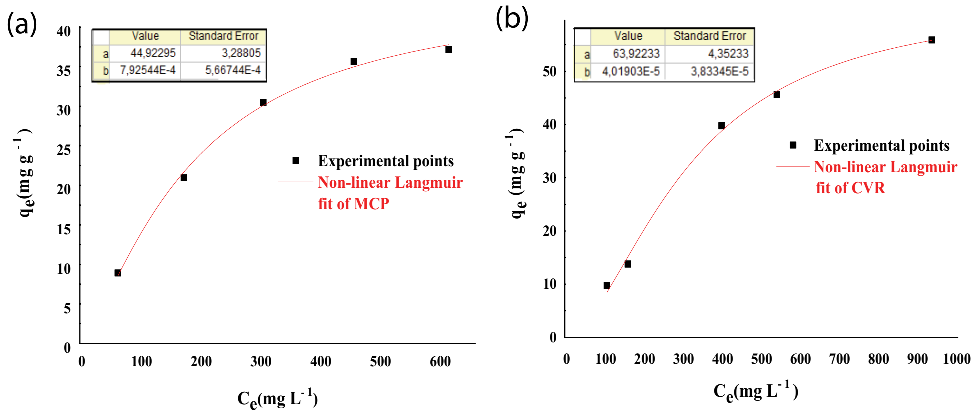

	Value	Standard Error
a	44,92295	3,28805
b	7,92544E-4	5,66744E-4

	Value	Standard Error
a	63,92233	4,35233
b	4,01903E-5	3,83345E-5

Fig. 9. Nonlinear form of the Langmuir isotherm for both types of biosorbents: (a) q_{max} (mg g^{-1}), (b) K_L (L mg^{-1})) (C_0 = [200–1,000] mg L^{-1}, pH = 5, agitation speed = 150 rpm, T = 25°C, biomass content: 10 g L^{-1}, granulometry: [0.315–0.4] mm, t = 3 h).

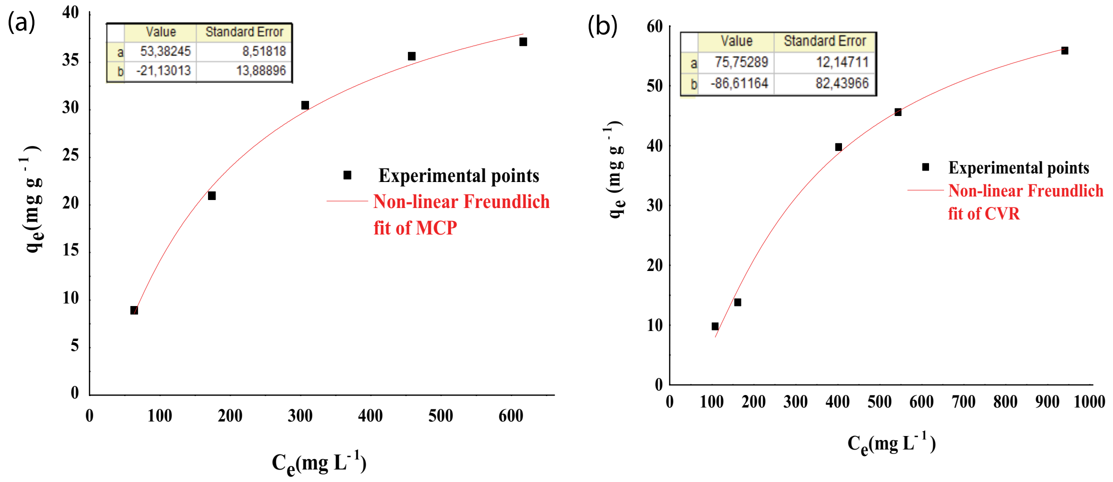

(a)

	Value	Standard Error
a	53,38245	8,51818
b	-21,13013	13,88896

(b)

	Value	Standard Error
a	75,75289	12,14711
b	-86,61164	82,43966

Fig. 10. Nonlinear form of the Freundlich isotherm for both types of biosorbents: (a) K_F (mg $^{(1-n)}$ L^n g^{-1}), (b) (1/n) (C_0 = [200–1,000] mg L^{-1}, pH = 5, agitation speed = 150 rpm, T = 25°C, biomass content : 10 g L^{-1}, granulometry: [0.315–0.4] mm, t = 3 h).

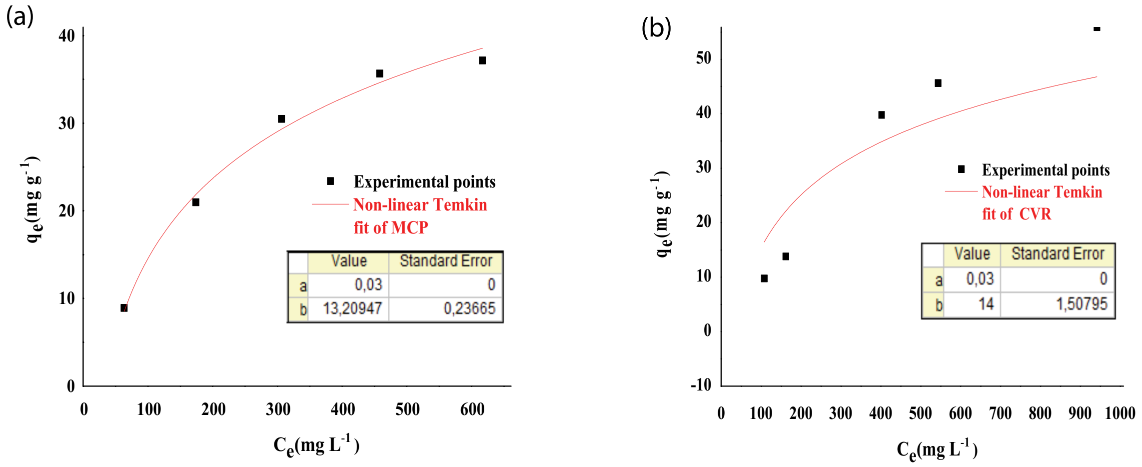

(a)

	Value	Standard Error
a	0,03	0
b	13,20947	0,23665

(b)

	Value	Standard Error
a	0,03	0
b	14	1,50795

Fig. 11. Nonlinear form of the Temkin isotherm for both types of biosorbents: (a) K_T (L mg^{-1}), (b) $\frac{RT}{\Delta Q}$) (C_0 = [200–1,000] mg L^{-1}, pH = 5, agitation speed = 150 rpm, T = 25°C, biomass content 10 g L^{-1}, granulometry: [0.315–0.4] mm, t = 3 h).

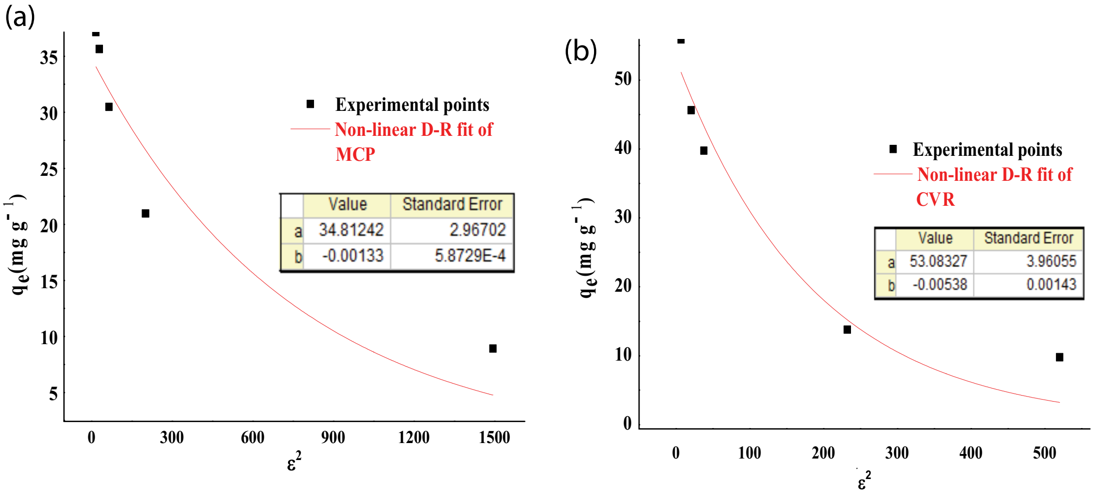

(a)

	Value	Standard Error
a	34.81242	2.96702
b	-0.00133	5.8729E-4

(b)

	Value	Standard Error
a	53.08327	3.96055
b	-0.00538	0.00143

Fig. 12. Nonlinear form of D-R isotherm for both types of biosorbents: (a) q_{mDR} (mg g^{-1}), (b) (BC_0 = [200–1,000] mg L^{-1}, pH = 5, agitation speed = 150 rpm, T = 25°C, biomass content: 10 g L^{-1}, granulometry: [0.315–0.4] mm, t = 3 h).

Table 7
Sorption capacities of different biosorbents for copper removal

Adsorbent	$q_{\max}$ (mg g^{-1})	Reference
Modified orange peel	50.25	[28]
Sugar beet pectin hydrogels	43.7	[20]
Modified orange peel	15.27	[45]
Sour orange peel	52.08	[30]
Pectin iron oxide magnetic nanocomposite	48.99	[56]
Modified orange peel	48.95	[24]
MCP	44.92	This study
CVR	63.92	This study

In this case, the values of the energy are positive and are in the order of 9.64 and 19.38 kJ mol^{-1} for CVR and MCP (Table 6). These results indicate that the mechanism of biosorption of copper ions is endothermic with chemical-type interactions in the knowledge that ion exchange and particle diffusion are the dominant mechanisms. The same results have been stated in previous studies for several types of biosorbents [20,45].

To confirm the accuracy of the models used, the results obtained in this study (Table 7) were compared with those reported for other biosorbents [20,24,28,30,45,56]. It was noticed that the maximum biosorption capacities of CVR (63.92 mg g^{-1}) and MCP (44.92 mg g^{-1}) are superior or comparable with the majority of the other ones. The differences observed can be attributed to different surface characteristics associated with the diversity of functional groups [57]. This indicates that the biosorbents used could be considered as promising materials for the removal of heavy metals from aqueous solutions.

4. Conclusion

The effectiveness of two prepared biosorbents (CVR and MCP) for the removal of Cu(II) ions from aqueous solutions was examined in this paper. An evaluation of parameters influencing the biosorption succeded in optimizing the following parameters: particle size (0.31–0.40 mm), biomass concentration (10 g L^{-1}), pH of the suspension (pH = 5.0), stirring speed (150 rpm), and contact time (3 h).

Several mathematical models were utilized to describe the equilibrium and kinetics of biosorption of copper ions on the surface of biosorbents. It was shown that under the optimal conditions, the maximum sorption capacity obtained by the nonlinear form of Langmuir model was found equal to 63.92 mg g^{-1} for CVR against a value of 44.92 mg g^{-1} recorded for MCP. Under the same conditions, the variation of the biosorption energy (ΔQ) resulting from the nonlinearization of the Temkin model was found positive and the sorption energy calculated by the D-R isotherm was found in the order of 9.64 kJ mol^{-1} for CVR and 19.38 kJ mol^{-1} for MCP, which indicates that the biosorption of Cu(II) on these biosorbents is endothermic. This also indicates that the interactions are of ion exchange type for CVR and of particle diffusion type for MCP.

Finally, it was shown that the kinetics of the biosorption is well described by employing the pseudo-second-order model for both types of biosorbents. The obtained results and their comparison with various biosorbents reported in previous works showed that CVR and MCP are effective biosorbents for the removal of copper ions and could be used for other heavy metals.

References

[1] M.R. Roger, Composite Materials from Agricultural Resources, Denmark Academy of Technical Science, Lyngby, 1995, pp. 27–41.
[2] R. Vinodhini, M. Narayanan, Bioaccumulation of heavy metals in organs of fresh water fish *Cyprinus carpio* (common carp), Int. J. Environ. Sci. Technol., 5 (2008) 179–182.
[3] A. Demirak, F. Yilmaz, A.L. Tuna, N. Ozdemir, Heavy metals in water, sediment and tissues of *Leuciscus cephalus* from a stream in southwestern Turkey, Chemosphere, 63 (2006) 1451–1458.
[4] U. Förstner, G.T.W. Wittmann, Metal Pollution in the Aquatic Environment, Springer, Heidelberg, Berlin, 1981.
[5] Y.M. Nor, Ecotoxicity of copper to aquatic biota: a review, Environ. Res., 43 (1987) 274–282.
[6] J.O. Duruibe, M.O.C. Ogwuegbu, J.N. Egwurugwu, Heavy metal pollution and human biotoxic effects, Int. J. Phys. Sci., 2 (2007) 112–118.
[7] C.C. Pfeiffer, R. Mailloux, Excess copper as a factor in human diseases, J. Orthomol. Med., 2 (1987) 171–182.
[8] A.G. EL Samrani, B.S. Lartiges, F. Villiéras, Chemical coagulation of combined sewer overflow: heavy metal removal and treatment optimization, J. Water Res., 42 (2008) 951–960.
[9] A. Bódalo-Santoyo, J.L. Gómez-Carrasco, E. Gómez-Gómez, F. Máximo-Martín, A.M. Hidalgo-Montesinos, Application of reverse osmosis to reduce pollutants present in industrial wastewater, Desalination, 155 (2003) 101–108.
[10] B. Zhang, H.-Z. Liu, W. Wang, Z.-G. Gao, Y.-H. Cao, Recovery of rhenium from copper leach solutions using ion exchange with weak base resins, Hydrometallurgy, 173 (2017) 50–56.
[11] D.J. Ennigrou, M.B.S. Ali, M. Dhahbi, Copper and zinc removal from aqueous solutions by polyacrylic acid assisted-ultrafiltration, Desalination, 343 (2014) 82–87.
[12] H. Demiral, C. Güngör, Adsorption of copper (II) from aqueous solutions on activated carbon prepared from grape bagasse, J. Clean Prod., 16 (2016) 959–6526.
[13] M.E. Argun, S. Dursun, Removal of heavy metal ions using chemically modified adsorbents, J. Int. Environ. Appl. Sci., 1 (2006) 27–40.
[14] J. He, J.P. Chen, A comprehensive review on biosorption of heavy metals by algal biomass: materials, performances, chemistry and modeling simulation tools, Bioresour. Technol., 160 (2014) 67–78.
[15] S. Babel, T.A. Kurniawan, Low-cost adsorbents for heavy metals uptake from contaminated water: a review, J. Hazard. Mater., 97 (2003) 219–243.
[16] D. Jedryczko, P. Pohl, M. Welna, Determination of the total cadmium, copper, lead and zinc concentrations and their labile species fraction in apple beverages by flow-through anodic stripping chronopotentiometry, Food Chem., 225 (2017) 220–229.
[17] R. Sudha, K. Srinivasan, P. Premkumar, Kinetic, mechanism and equilibrium studies on removal of Pb(II) using Citrus limettioides peel and seed carbon, Res. Chem. Intermed., 42 (2016) 1677–1697.
[18] F.A. Pavan, I.S. Lima, E.C. Lima, C. Airoldi, Y. Gushikem, Use of ponkan mandarin peels as biosorbent for toxic metals uptake from aqueous solutions, J. Hazard. Mater., 137 (2006) 527–533.
[19] M. Kiliç, M.E. Keskin, S. Mazlum, N. Mazlum, Effect of conditioning for Pb(II) and Hg(II) biosorption on waste activated sludge, Chem. Eng. Process, 47 (2008) 31–40.
[20] Y.N. Mata, M.L. Blázquez, A. Ballester, F. González, J.A. Muñoz, Sugar-beet pulp pectin gels as biosorbent for heavy metals:

preparation and determination of biosorption and desorption characteristics, Chem. Eng. J., 150 (2009) 289–301.

[21] W.E. Marshall, L.H. Wartelle, D.E. Boler, M.M. Johns, C.A. Toles, Enhanced metal adsorption by soybean hulls with citric acid, Bioresour. Technol., 69 (1999) 263–268.

[22] L.H. Wartelle, W.E. Marshall, Citric acid modified agricultural by-products as copper ion adsorbents, Adv. Environ. Res., 4 (2000) 1–7.

[23] M.K. Sahu, S. Mandal, S.S. Dash, P. Badhai, R.K. Patel, Removal of Pb(II) from aqueous solution by acid activated red mud, J. Environ. Chem. Eng., 1 (2013) 1315–1324.

[24] L.A. Romero-Cano, H. García-Rosero, L.V. Gonzalez-Gutiérrez, L.A. Baldenegro-Pérez, F. Carrasco-Marín, Functionalized adsorbents prepared from fruit peels: equilibrium, kinetic and thermodynamic studies for copper adsorption in aqueous solution, J. Clean Prod., 162 (2017) 195–204.

[25] S. Hoo Lee, C.H. Jung, H. Chung, M.Y. Lee, J-W. Yang, Removal of heavy metals from aqueous solutions by apple residues, Process Biochem., 33 (1998) 205–211.

[26] G.S. Dhillon, S. Kaur, S.K. Brar, Perspective of apple processing wastes as low-cost substrates for bioproduction of high value products: a review, Renew. Sust. Energ. Rev., 27 (2013) 789–805.

[27] https://fr.actualitix.com/pays/dza/algerie-pomme-production.php.

[28] N.-C. Feng, X.-Y. Gue, S. Liang, Enhanced Cu(II) adsorption by orange peel modified with sodium hydroxide, T. Nonferr. Metal Soc., 20 (2010) s146–s152.

[29] A.O. Dada, A.P. Olalekan, A.M. Olatunya, O. Dada, Langmuir, Freundlich, Temkin and Dubinin–Radushkevich isotherms studies of equilibrium sorption of Zn^{2+} unto phosphoric acid modified rice husk, J. Appl. Chem., 3 (2012) 38–45.

[30] M. Khormaei, B. Nasernejad, M. Edrisi, T. Eslamzadeh, Copper biosorption from aqueous solutions by sour orange residue, J. Hazard. Mater., 149 (2007) 269–274.

[31] S. Larous, A.H. Meniai, Adsorption of diclofenac from aqueous solution using activated carbon prepared from olive stones, Int. J. Hydrogen Energy, 41 (2016) 10380–10390.

[32] A. Tassist, H. Lounici, N. Abdi, N. Mameri, Equilibrium, kinetic and thermodynamic studies on aluminium biosorption by a mycelial biomass (*Streptomyces rimosus*), J. Hazard. Mater., 183 (2010) 35–43.

[33] M.A. Martín-Lara, G. Blázquez, M. Calero, A.I. Almendros, A. Ronda, Binary biosorption of copper and lead onto pine cone shell in batch reactors and in fixed bed columns, Int. J. Miner. Process, 148 (2016) 72–82.

[34] A. Zubair, H.N. Bhatti, M.A. Hanif, F. Shafqat, Kinetic and equilibrium modeling for Cr(III) and Cr(VI) removal from aqueous solutions by citrus reticulata waste biomass, Water Air Soil Pollut., 191 (2008) 305–318.

[35] J. Lin, L. Wang, Comparison between linear and non-linear forms of pseudo-first-order and pseudo-second-order adsorption kinetic models for the removal of methylene blue by activated carbon, Front. Environ. Sci. Eng., 3 (2009) 320–324.

[36] H. Yu, J. Pang, T. Ai, L. Liu, Biosorption of Cu^{2+}, Co^{2+} and Ni^{2+} from aqueous solution by modified corn silk: equilibrium, kinetics and thermodynamic studies, J. Taiwan Inst. Chem. Eng., 62 (2016) 21–30.

[37] S. Shahmohammadi-Kalalagh, H. Babazadeh, A. Nazmi, Comparison of linear and nonlinear forms of isotherm models for Zn(II) and Cu(II) sorption on a kaolinite, Arabian J. Geosci., 8 (2015) 397–402.

[38] K.A. Shroff, V.K. Vaidya, Kinetics and equilibrium studies on biosorption of nickel from aqueous solution by dead fungal biomass of Mucorhiemalis, Chem. Eng. J., 171 (2011) 1234–1245.

[39] S. Dutta, A. Bhattacharyya, A. Ganguly, S. Gupta, S. Basu, Application of response surface methodology for preparation of low cost adsorbent from citrus fruit peel and for removal of methylene blue, Desalination, 275 (2011) 26–36.

[40] J.N. Sahu, J. Acharya, B.C. Meikap, Response surface modeling and optimization of chromium (vi) removal from aqueous solution using tamarind wood activated carbon in batch process, J. Hazard. Mater., 172 (2009) 818–825.

[41] A. Bhatnagar, M. Sillanpää, A. Witek-Krowiak, Agricultural waste peels as versatile biomass for water purification − a review, Chem. Eng. J., 270 (2015) 244–271.

[42] X. Li, Y. Tang, X. Cao, D. Lu, F. Luo, W. Shao, Preparation and evaluation of orange peel cellulose adsorbents for effective removal of cadmium, zinc, cobalt and nickel, Colloids Surf. A Physicochem. Eng. Asp., 317 (2008) 512–521.

[43] V. Lugo-Lugo, S. Hernandez-Lopez, C. Barrera-Diaz, F. Urena-Nunez, B. Bilyeu, A comparative study of natural, formaldehyde-treated and copolymer-grafted orange peel for pb(II) adsorption under batch and continuous mode, J. Hazard. Mater., 161 (2009) 1255–1264.

[44] M.A. Wahab, S. Jellali, N. Jedidi, Ammonium biosorption onto sawdust: FTIR analysis, kinetics and adsorption isotherms modelling, Bioresour. Technol., 101 (2010) 5070–5075.

[45] M.R. Lasheen, N.S. Ammar, H.S. Ibrahim, Adsorption/desorption of Cd(II),Cu(II) and pb(II) using chemically modified orange peel: equilibrium and kinetic studies, Solid State Sci., 14 (2012) 202–210.

[46] A.H. Ören, A. Kaya, Factors affecting adsorption characteristics of Zn^{2+} on two natural zeolites, J. Hazard. Mater., 131 (2006) 59–65.

[47] R.L. Ramos, G.A. Armenta, L.V. Gonzalez-Gutierrez, R.M. Guerrero-Coronado, J. Mendoza-Barron, Ammonia exchange on clinoptilolite from mineral deposits located in Mexico, J. Chem. Technol. Biotechnol., 79 (2004) 651–657.

[48] U.A. Guler, M. Sarioglu, Single and binary biosorption of Cu(II), Ni(II) and methylene blue by raw and pretreated *Spirogyra* sp.: equilibrium and kinetic modelling, J. Environ. Chem. Eng., 1 (2013) 369–377.

[49] M. Izquierdo, P. Marzal, P.N.L. Lens, effect of organic ligands on copper (II) removal from metal plating waste water by orange peel based biosorbents, Water Air Soil Pollut., 224 (2013) 1507–1522.

[50] M. Omraei, H. Esfandian, R. Katal, M. Ghorbani, Study of the removal of Zn(II) from aqueous solution using polyrrole nanocomposite, Desalination, 271 (2011) 248–256.

[51] T.J. Mohammed, R.I. Ibrahim, Remediation of Cu(II) from well water of Iraq by using cortex of fruits and agricultural waste, Arabian J. Sci. Eng., 41 (2016) 345–355.

[52] M. Kazmi, N. Feroze, S. Naveed, S.H. Javed, Biosorption of copper(II) on prunus amygdalus shell: characterization, biosorbent size analysis, kinetic, equilibrium and mechanistic studies, Korean J. Chem. Eng., 28 (2011) 2033–2040.

[53] X. Chen, Modeling of experimental adsorption isotherm data, Information, 6 (2015) 14–22.

[54] J. Hu, S.W. Wang, D.D. Shao, Y.H. Dong, J.X. Li, X.K. Wang, Adsorption and reduction of chromium (VI) from aqueous solution by multiwalled carbon nanotubes, Open Environ. Pollut. Toxicol. J., 1 (2009) 66–73.

[55] D. Xu, X.L. Tan, C.L. Chen, X.K. Wang, Adsorption of Pb(II) from aqueous solution to MX-80 bentonite: effect of pH, ionic strength, foreign ions and temperature, Appl. Clay Sci., 41 (2008) 37–46.

[56] J.L. Gong, X.Y. Wang, G.M. Zeng, L. Chen, J.H. Deng, X.R. Zhang, Q.Y. Niu, Copper (II) removal by pectin–iron oxide magnetic nanocomposite adsorbent, Chem. Eng. J., 185–186 (2012) 100–107.

[57] S. Srivastava, S.B. Agrawal, M.K. Mondal, A review on progress of heavy metal removal using adsorbents of microbial and plant origin, Environ. Sci. Pollut. Res. Int., 22 (2015) 15386–15415.